JACS
JOURNAL OF THE AMERICAN CHEMICAL SOCIETY
Communication
pubs.acs.org/JACS

Solution Structures of Highly Active Molecular Ir Water-Oxidation Catalysts from Density Functional Theory Combined with High-Energy X-ray Scattering and EXAFS Spectroscopy

Ke R. Yang,[†] Adam J. Matula,[†] Gihan Kwon,[‡] Jiyun Hong,[§] Stafford W. Sheehan,[†,⊥] Julianne M. Thomsen,[†] Gary W. Brudvig,[†] Robert H. Crabtree,[†] David M. Tiede,[‡] Lin X. Chen,[‡,§] and Victor S. Batista*[,†]

[†]Yale Energy Sciences Institute and Department of Chemistry, Yale University, New Haven, Connecticut 06520-8107, United States
[‡]Chemical Sciences and Engineering Division, Argonne National Laboratory, Argonne, Illinois 60439, United States
[§]Department of Chemistry, Northwestern University, 2145 Sheridan Road, Evanston, Illinois 60208-3113, United States

Supporting Information

ABSTRACT: The solution structures of highly active Ir water-oxidation catalysts are elucidated by combining density functional theory, high-energy X-ray scattering (HEXS), and extended X-ray absorption fine structure (EXAFS) spectroscopy. We find that the catalysts are Ir dimers with mono-μ-O cores and terminal anionic ligands, generated in situ through partial oxidation of a common catalyst precursor. The proposed structures are supported by ^{1}H and ^{17}O NMR, EPR, resonance Raman and UV−vis spectra, electrophoresis, etc. Our findings are particularly valuable to understand the mechanism of water oxidation by highly reactive Ir catalysts. Importantly, our DFT-EXAFS-HEXS methodology provides a new in situ technique for characterization of active species in catalytic systems.

Understanding catalytic systems for water oxidation is the most challenging aspect of artificial photosynthesis, the fundamental chemical process that extracts reducing equivalents (i.e., electrons) from water to generate fuels.[1,2] Half-sandwich Cp*Ir^{III} (Cp* = pentamethyl-cyclopentadienyl) complexes have been developed, serving as effective precatalysts for water oxidation.[3] However, the actual catalytic species formed by oxidative transformation of the Cp*Ir^{III} precatalyst have remained elusive, in spite of repeated efforts to crystallize the catalyst resting states.[4−22] The outstanding challenge is thus to elucidate the concentration-dependent structure of the active species present in solution, which is vital to understand the underlying catalytic mechanism that could form the basis for the rational design of more efficient and robust catalysts for water oxidation.

When X-ray diffraction results are not available, extended X-ray absorption fine structure (EXAFS) provides a useful approach to characterize the ligand environment around metal atoms, as in the case for Ru,[23,24] Co,[25,26] and Mn[27] catalysts for water oxidation. Pair distribution function (PDF) analysis from high-energy X-ray scattering (HEXS) provides an important complement to XAFS studies, including first shell, outer sphere, and longer range distances that are not directly accessible by EXAFS.[28,29] Density functional theory (DFT) yields structural and energetic information that can be used to simulate EXAFS and PDF data to elucidate the active species in catalytic systems by comparison to experimental results.

Here, we characterize the solution structure of an active Ir species by combining DFT studies with HEXS and EXAFS spectroscopy data. We analyze the complexes by DFT calculations and direct comparisons to spectroscopic data, using the B3LYP functional[30] as implemented in the Gaussian 09 software package.[31] Solvation effects are considered using the PCM solvation model[32] and the dispersion interactions by Grimme's D2 correction.[33] EXAFS spectra of the DFT optimized structures are simulated using the codes FEFF (version 8.30)[34] and IFEFFIT,[35] while the HEXS spectra are simulated as previously described.[15] Details of the computational methods are provided in the SI.

Clear evidence that the Cp* ligand undergoes oxidative degradation comes from the formation of CH_3COOH, HCOOH, CO_2, and glycolic acid ($HOCH_2COOH$), depending on the sacrificial oxidants and reaction conditions.[8,14,22] Importantly, chelating ligands and low solution concentrations are necessary to prevent nanoparticle formation during activation of Cp*Ir^{III} complexes with $NaIO_4$.[11] A stable blue species, able to catalyze O_2 evolution by water oxidation, is formed in solution when precatalyst **1** (Chart 1) is activated by $NaIO_4$ with release of ∼1.8 equiv acetic acid.[18] Precatalyst **1** can also be activated electrochemically at 1.4 V after 36 h, resulting in a similarly active stable blue solution.[20] Anchoring the chemically activated blue-

Chart 1. Catalyst Precursor (1) and Proposed Active Species in Chemically (2), and Electrochemically (3) Activated Ir Blue Solutions

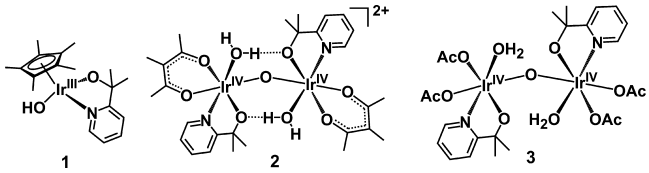

1 2 3

Received: February 17, 2016
Published: April 18, 2016

DOI: 10.1021/jacs.6b01750
J. Am. Chem. Soc. 2016, 138, 5511−5514

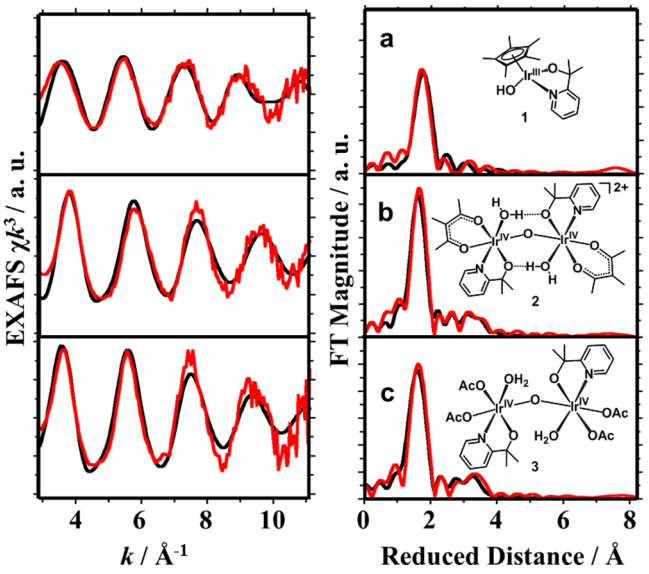

Figure 1. Experimental (red) and calculated (black) EXAFS spectra of the catalyst precursor (a), chemically (b), and electrochemically (c) activated Ir blue-solution species, in k space (left) and reduced distance space (right).

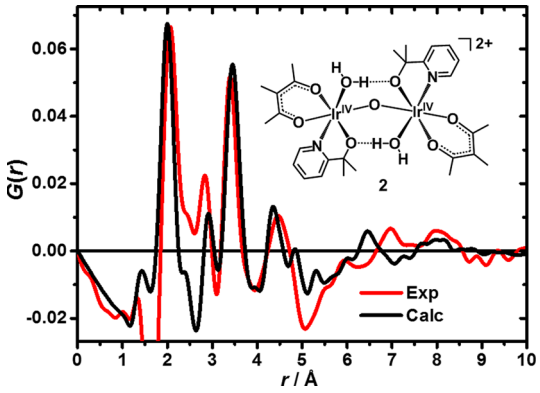

Figure 2. Experimental and calculated electron density pair distribution function, $G(r)$, for the chemically activated Ir blue-solution species.

solution species to metal oxides yields a heterogenized molecular catalyst for water oxidation that has activity and stability comparable to state-of-the-art bulk metal oxide catalysts.[36] However, since isolation and crystallization of the pure active species from aqueous solution has thus far proven to be impossible, no X-ray diffraction data are available.[37]

Activation of the precatalyst **1** with $NaIO_4$ shows decomposition of Cp*. The color change of the solution, from orange to blue, suggests that the Ir centers have been oxidized from Ir(III) to open-shell Ir(IV), while ^{1}H NMR data indicate the pyalc (pyalc = 2-(2′pyridyl)-2-propanolate) ligand is retained. XPS study suggests Ir is exclusively in the (IV) oxidation state. Resonance Raman (RR) data suggest the presence of μ-O ligands, while ^{17}O NMR data show that the ratio of terminal aqua to μ-O ligands is 2:1. EPR study suggests the active species should be a singlet, and MALTI-TOF MS suggests an Ir−O−Ir core structure of the active species. Finally, an electrophoretic study shows a cationic complex is present since the blue species moves toward the cathode uniformly. Based on the above experimental results, a bis-μ-O Ir dimer structure has been proposed: $[(pyalc)(H_2O)_2Ir^{IV}(\mu\text{-}O)_2Ir^{IV}(OH_2)_2(pyalc)]^{2+}$.[18] However, that bis-$\mu$-O model is inconsistent with the newly obtained experimental EXAFS (Figure S7). Here, we find that mono-μ-O Ir^{IV} dimer models, including complexes **2** and **3** in Chart 1, fit as active species in the chemically and electrochemically activated Ir blue solutions, respectively.

The simulated EXAFS spectrum of precursor **1** agrees well the experimental results (Figure 1a), which validates our approach of DFT-EXAFS to determine the ligand environment of transition-metal complexes. Simulation of the originally proposed structure indicated that a di-μ-O Ir dimer model has an Ir−Ir distance that is too short to fit with the EXAFS and HEXS data shown in Figures 1 and 2, respectively, necessitating a mono-μ-O Ir dimer model for solutions prepared under the conditions that HEXS measurements were made. For such a model to be consistent with the 10 mM ^{17}O NMR results,[18] there needs to be two terminal aqua ligands for the chemically active species, one per Ir center. This leaves two coordination sites to be filled by other ligands present in the solution. Because acetic acid and IO_3^- are known to be present in the chemically activated Ir blue solution,[18] we considered various binding modes of AcO^- and IO_3^- across a large number of possible isomers. None of them yielded EXAFS spectra consistent with experimental spectra (see SI for full comparison). However, when we considered 2-methyl-2-acetyl acetonate (macac) as the chelating ligand, we obtained a very good match with the simulated and experimental EXAFS in both k space and reduced distance space (Figure 1b). Macac can be generated from the oxidation of Cp*, leaving two CH_3−C units to be oxidized to AcOH, consistent with experimental observation that ∼1.8 equiv AcOH are released into solution. Additionally, we posit that the unidentified signal found around 1.7 ppm in ^{1}H NMR[18] can be attributed to the CH_3 group in macac (Figure S23). After repeated catalytic turnovers, as occur during electrochemical activation, macac may be replaced by acetate due to its oxidative susceptibility.

The experimental EXAFS spectrum of the electrochemically activated Ir blue solution was also modeled. The electrochemical activation of precatalyst **1** by bulk electrolysis in Na_2SO_4-containing electrolyte introduces AcO^- into the solution. Thus, we considered AcO^- and SO_4^{2-} as possible ligands around the Ir centers. Only the simulated EXAFS spectra of the model with AcO^- binding as a monodentate ligand to the mono-μ-O Ir dimer adequately reproduced the experimental EXAFS results (Figure 1c). See the SI for the exhaustive list of isomers considered and comparisons of each with the experimental spectra. Our DFT optimized bond distances of complexes **2** and **3** agree well with the bond lengths extracted from experimental EXAFS spectra (Tables S13−14), further confirming the reliability of our models.

We also studied HEXS for the chemically activated Ir solution and compared the experiment-derived PDF, $G(r)$, with the calculated $G(r)$ from our DFT-optimized structure **2**, presented in Figure 2. Our calculated $G(r)$ reproduces the experimental $G(r)$ quite well when $r < 6$ Å. This is sufficient to identify the Ir-μ-oxo-Ir bonding pattern and dimeric nature of the active species. We note that complex **3**, which has ligand environment and EXAFS spectra similar to **2**, can be distinguished with HEXS (Figure S33). By analyzing the calculated $G(r)$, four peaks at 2.0, 2.9, 3.4, and 4.5 Å could be assigned to Ir−O/Ir−N in the first coordination shell, Ir−C in the second coordination shell, and Ir−Ir and Ir−O distances as well as the distances between Ir and C in the macac and pyalc group. Although heterogeneous amorphous deposits may be formed at the high concentrations (20 mM) at which our HEXS measurements were made, our

DOI: 10.1021/jacs.6b01750
J. Am. Chem. Soc. 2016, 138, 5511−5514

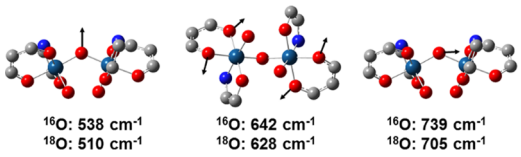

Figure 3. Calculated Raman-active modes and frequency shift with $^{18}O/^{16}O$ substitution (only Ir, O (red), N (blue)) and C atoms (gray) in macac are shown for clarity).

HEXS results suggest the dominant species are molecular Ir species. It is possible to consider model refinement to achieve better agreement beyond 6 Å. These distances involve outer shell ligand atoms which are influenced by ligand conformation and interactions with solvent molecules. Explicit water molecules were not included in the present DFT analysis, and further conformational modeling could be done. However, a key finding of the present study is that DFT-EXAFS-HEXS approach identifies an Ir−μ-O−Ir active species which would not be affected by these refinements. This is distinct from a Ir−$(\mu\text{-O})_2$−Ir pattern proposed previously[18] and also invoked for a catalyst derived from a different IrCp* precursor complex.[38]

While the EXAFS and HEXS results provide strong support for the model with mono-μ-O Ir dimers for both chemical and electrochemical preparations of the active Ir species, the original study also reported RR and UV−vis spectra so we simulated these for the new models to confirm viability. The RR studies have shown that three RR peaks at 559, 610, and 666 cm^{-1} are observed when excited at 660 nm (5 mM concentration).[18] These peaks shift to 538, 577, and 610 cm^{-1} when complex **1** is activated in $^{18}OH_2$. This experimental evidence was used to demonstrate the possibility of bis-μ-O Ir^{IV} dimers since DFT results of the bis-μ-O model showed four Raman-active vibration modes with vibrational frequencies of 525, 532, 717, and 722 cm^{-1} corresponding to the vibrations of the Ir_2O_2 core and these vibrational frequencies show a shift of 28−41 cm^{-1} after $^{18}O/^{16}O$ substitution. For complex **2**, our calculations predict three Raman-active modes at 538, 642, and 739 cm^{-1}. After $^{18}O/^{16}O$ substitution, those modes shift to 510, 628, and 705 cm^{-1} (Figure 3). Our results suggest that the previous RR spectral data may be more consistent with our mono-μ-O model.

The available UV−vis data also support our model. Under acidic conditions, the terminal ligands are protonated as aqua ligands, and the chemically activated Ir species has a maximum absorption at 608 nm.[18] When this solution is basified with NaOH, the maximum absorption blue shifts to 590 nm since the terminal ligands are deprotonated to OH^-. Our time-dependent DFT (TDDFT) calculations give a similar trend. Our simulated UV−vis spectra have peak absorptions at 632 nm for the **2**-OH_2 form and at 613 nm with a blue shift of 19 nm (0.06 eV) for the **2**-OH form, in excellent agreement with the experimental observation (Table 1).

Our proposed structure for the active catalyst of the recently developed Ir catalysts is consistent with the newly available EXAFS and HEXS results as well as previous experimental results. The model structures we propose are mono-μ-O Ir dimers with chelating pyalc and one aqua ligand coordinating to each Ir atom as well as two sites coordinated by anionic ligands (such as macac, AcO^-, and possibly $^-OOCCH_2CH_2COO^-$ when activated from a [(cod)Ir^I(pyalc)] precursor).[18] Our model structures represent a family of active catalysts for water oxidation with mono-μ-O Ir dimers that resemble the well characterized Ru blue dimer.[39]

Table 1. Experimental and Calculated Absorption Wave Length (in nm) and Excitation Energies (in eV)

	expt	calcd
2-OH_2	608 (2.04)	632 (1.96)
2-OH	590 (2.10)	613 (2.02)

Scheme 1. Proposed Pathway of O_2 Evolution Catalyzed by Ir Water Oxidation Catalysts

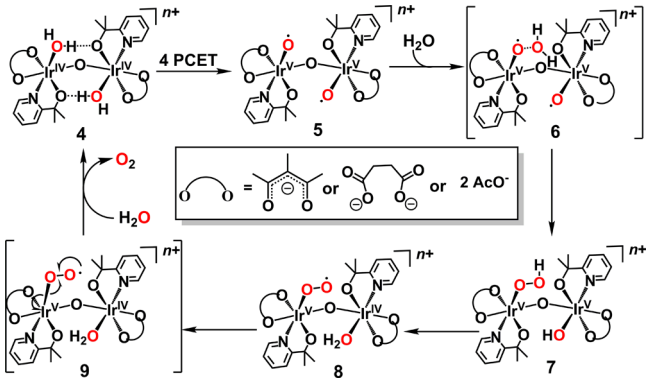

With the structures of the active catalyst available, a pathway of the O_2 evolution catalyzed by Ir catalysts can now be proposed (Scheme 1). The catalytic cycle begins with four proton-coupled electron-transfer steps to form an oxidized intermediate **5**. This intermediate could undergo nucleophilic attack by OH_2 through transition state **6** to form the hydroperoxo complex **7**. An intramolecular proton-coupled electron transfer could occur resulting in the superoxo complex **8**, which could evolve O_2 by Ir−O bond cleavage through transition state **9**. Finally, a water molecule replaces O_2 to regenerate catalyst **4** and release O_2. The proposed mechanism resembles the well-studied pathway of O_2 evolution catalyzed by the Ru blue dimer which is similar in structure to the proposed active catalyst.[1,23,40,41]

In conclusion, we find a mono-μ-O di-Ir model for the active species in both chemically and electrochemically activated blue solutions consistent with our EXAFS and HEXS data as well as ^1H and ^{17}O NMR, RR and UV−vis spectra, electrophoresis, etc. Both the structures we obtain and our proposed catalytic pathway for water oxidation resemble those for the well-characterized Ru blue dimer. Our model provides new insight into the mechanism of water oxidation by these robust, highly active Ir complexes, which in turn lays the groundwork for the rational design of even more efficient catalysts. Our results demonstrate the ability of the DFT-EXAFS-HEXS method to characterize active species in crude reaction mixtures of catalytic systems.

■ ASSOCIATED CONTENT

Supporting Information

The Supporting Information is available free of charge on the ACS Publications website at DOI: 10.1021/jacs.6b01750.

Computational and experimental details and data (PDF)

■ AUTHOR INFORMATION

Corresponding Author

*victor.batista@yale.edu

DOI: 10.1021/jacs.6b01750
J. Am. Chem. Soc. 2016, 138, 5511−5514

Present Address

[⊥]Catalytic Innovations LLC, 70 Crandall Road, PO Box 356, Adamsville, Rhode Island, 02801, United States.

Notes

The authors declare the following competing financial interest(s): U.S. patent application no. 14/317,906 by S.W.S., J.M.T., R.H.C., and G.W.B. contains intellectual property on the Ir water oxidation catalytic systems described in this article.

■ ACKNOWLEDGMENTS

This work was supported as part of the Argonne-Northwestern Solar Energy Research (ANSER) Center, an Energy Frontier Research Center funded by the U.S. Department of Energy, Office of Science, Office of Basic Energy Sciences (US DOE-OS-BES) under award no. DE-SC0001059. X-ray measurements were carried out at the Advanced Photon Source, operated by Argonne National Laboratory for the US DOE-OS-BES under contract no. DE-AC02-06CH11357. D.M.T. acknowledges DOE BES program support for the model-based calculation of PDF data under this Laboratory Contract. We thank the National Energy Research Scientific Computing Center (NERSC) and Yale High Performance Computation Center for generous computer time allocations.

■ REFERENCES

(1) Kärkäs, M. D.; Verho, O.; Johnston, E. V.; Åkermark, B. *Chem. Rev.* **2014**, *114*, 11863.
(2) Blakemore, J. D.; Crabtree, R. H.; Brudvig, G. W. *Chem. Rev.* **2015**, *115*, 12974.
(3) Hull, J. F.; Balcells, D.; Blakemore, J. D.; Incarvito, C. D.; Eisenstein, O.; Brudvig, G. W.; Crabtree, R. H. *J. Am. Chem. Soc.* **2009**, *131*, 8730.
(4) Blakemore, J. D.; Schley, N. D.; Balcells, D.; Hull, J. F.; Olack, G. W.; Incarvito, C. D.; Eisenstein, O.; Brudvig, G. W.; Crabtree, R. H. *J. Am. Chem. Soc.* **2010**, *132*, 16017.
(5) Lalrempuia, R.; McDaniel, N. D.; Müller-Bunz, H.; Bernhard, S.; Albrecht, M. *Angew. Chem., Int. Ed.* **2010**, *49*, 9765.
(6) Savini, A.; Bellachioma, G.; Ciancaleoni, G.; Zuccaccia, C.; Zuccaccia, D.; Macchioni, A. *Chem. Commun.* **2010**, *46*, 9218.
(7) Grotjahn, D. B.; Brown, D. B.; Martin, J. K.; Marelius, D. C.; Abadjian, M.-C.; Tran, H. N.; Kalyuzhny, G.; Vecchio, K. S.; Specht, Z. G.; Cortes-Llamas, S. A.; Miranda-Soto, V.; van Niekerk, C.; Moore, C. E.; Rheingold, A. L. *J. Am. Chem. Soc.* **2011**, *133*, 19024.
(8) Savini, A.; Belanzoni, P.; Bellachioma, G.; Zuccaccia, C.; Zuccaccia, D.; Macchioni, A. *Green Chem.* **2011**, *13*, 3360.
(9) Hetterscheid, D. G. H.; Reek, J. N. H. *Chem. Commun.* **2011**, *47*, 2712.
(10) Bucci, A.; Savini, A.; Rocchigiani, L.; Zuccaccia, C.; Rizzato, S.; Albinati, A.; Llobet, A.; Macchioni, A. *Organometallics* **2012**, *31*, 8071.
(11) Hintermair, U.; Hashmi, S. M.; Elimelech, M.; Crabtree, R. H. *J. Am. Chem. Soc.* **2012**, *134*, 9785.
(12) Hong, D.; Murakami, M.; Yamada, Y.; Fukuzumi, S. *Energy Environ. Sci.* **2012**, *5*, 5708.
(13) Vagnini, M. T.; Smeigh, A. L.; Blakemore, J. D.; Eaton, S. W.; Schley, N. D.; D'Souza, F.; Crabtree, R. H.; Brudvig, G. W.; Co, D. T.; Wasielewski, M. R. *Proc. Natl. Acad. Sci. U. S. A.* **2012**, *109*, 15651.
(14) Zuccaccia, C.; Bellachioma, G.; Bolaño, S.; Rocchigiani, L.; Savini, A.; Macchioni, A. *Eur. J. Inorg. Chem.* **2012**, *2012*, 1462.
(15) Blakemore, J. D.; Mara, M. W.; Kushner-Lenhoff, M. N.; Schley, N. D.; Konezny, S. J.; Rivalta, I.; Negre, C. F. A.; Snoeberger, R. C.; Kokhan, O.; Huang, J.; Stickrath, A.; Tran, L. A.; Parr, M. L.; Chen, L. X.; Tiede, D. M.; Batista, V. S.; Crabtree, R. H.; Brudvig, G. W. *Inorg. Chem.* **2013**, *52*, 1860.
(16) Badia-Bou, L.; Mas-Marza, E.; Rodenas, P.; Barea, E. M.; Fabregat-Santiago, F.; Gimenez, S.; Peris, E.; Bisquert, J. *J. Phys. Chem. C* **2013**, *117*, 3826.
(17) Codolà, Z.; M, S.; Cardoso, J.; Royo, B.; Costas, M.; Lloret-Fillol, J. *Chem. - Eur. J.* **2013**, *19*, 7203.
(18) Hintermair, U.; Sheehan, S. W.; Parent, A. R.; Ess, D. H.; Richens, D. T.; Vaccaro, P. H.; Brudvig, G. W.; Crabtree, R. H. *J. Am. Chem. Soc.* **2013**, *135*, 10837.
(19) Lewandowska-Andralojc, A.; Polyansky, D. E.; Wang, C.-H.; Wang, W.-H.; Himeda, Y.; Fujita, E. *Phys. Chem. Chem. Phys.* **2014**, *16*, 11976.
(20) Thomsen, J. M.; Sheehan, S. W.; Hashmi, S. M.; Campos, J.; Hintermair, U.; Crabtree, R. H.; Brudvig, G. W. *J. Am. Chem. Soc.* **2014**, *136*, 13826.
(21) Woods, J. A.; Lalrempuia, R.; Petronilho, A.; McDaniel, N. D.; Muller-Bunz, H.; Albrecht, M.; Bernhard, S. *Energy Environ. Sci.* **2014**, *7*, 2316.
(22) Zuccaccia, C.; Bellachioma, G.; Bortolini, O.; Bucci, A.; Savini, A.; Macchioni, A. *Chem. - Eur. J.* **2014**, *20*, 3446.
(23) Moonshiram, D.; Jurss, J. W.; Concepcion, J. J.; Zakharova, T.; Alperovich, I.; Meyer, T. J.; Pushkar, Y. *J. Am. Chem. Soc.* **2012**, *134*, 4625.
(24) Okamoto, K.; Miyawaki, J.; Nagai, K.; Matsumura, D.; Nojima, A.; Yokoyama, T.; Kondoh, H.; Ohta, T. *Inorg. Chem.* **2003**, *42*, 8682.
(25) Risch, M.; Khare, V.; Zaharieva, I.; Gerencser, L.; Chernev, P.; Dau, H. *J. Am. Chem. Soc.* **2009**, *131*, 6936.
(26) Kanan, M. W.; Yano, J.; Surendranath, Y.; Dincă, M.; Yachandra, V. K.; Nocera, D. G. *J. Am. Chem. Soc.* **2010**, *132*, 13692.
(27) Mattioli, G.; Zaharieva, I.; Dau, H.; Guidoni, L. *J. Am. Chem. Soc.* **2015**, *137*, 10254.
(28) Du, P.; Kokhan, O.; Chapman, K. W.; Chupas, P. J.; Tiede, D. M. *J. Am. Chem. Soc.* **2012**, *134*, 11096.
(29) Huang, J.; Blakemore, J. D.; Fazi, D.; Kokhan, O.; Schley, N. D.; Crabtree, R. H.; Brudvig, G. W.; Tiede, D. M. *Phys. Chem. Chem. Phys.* **2014**, *16*, 1814.
(30) Stephens, P. J.; Devlin, F. J.; Chabalowski, C. F.; Frisch, M. J. *J. Phys. Chem.* **1994**, *98*, 11623.
(31) Frisch, M. J.; Trucks, G. W.; Schlegel, H. B.; Scuseria, G. E.; Robb, M. A.; Cheeseman, J. R.; Scalmani, G.; Barone, V.; Mennucci, B.; Petersson, G. A.; Nakatsuji, H.; Caricato, M.; Li, X.; Hratchian, H. P.; Izmaylov, A. F.; Bloino, J.; Zheng, G.; Sonnenberg, J. L.; Hada, M.; Ehara, M.; Toyota, K.; Fukuda, R.; Hasegawa, J.; Ishida, M.; Nakajima, T.; Honda, Y.; Kitao, O.; Nakai, H.; Vreven, T.; Montgomery, J. A., Jr.; Peralta, J. E.; Ogliaro, F.; Bearpark, M.; Heyd, J. J.; Brothers, E.; Kudin, K. N.; Staroverov, V. N.; Kobayashi, R.; Normand, J.; Raghavachari, K.; Rendell, A.; Burant, J. C.; Iyengar, S. S.; Tomasi, J.; Cossi, M.; Rega, N.; Millam, J. M.; Klene, M.; Knox, J. E.; Cross, J. B.; Bakken, V.; Adamo, C.; Jaramillo, J.; Gomperts, R.; Stratmann, R. E.; Yazyev, O.; Austin, A. J.; Cammi, R.; Pomelli, C.; Ochterski, J. W.; Martin, R. L.; Morokuma, K.; Zakrzewski, V. G.; Voth, G. A.; Salvador, P.; Dannenberg, J. J.; Dapprich, S.; Daniels, A. D.; Farkas, Ö.; Foresman, J. B.; Ortiz, J. V.; Cioslowski, J.; Fox, D. J. *Gaussian 09*, Rev. D01; Gaussian, Inc.: Wallingford, CT, 2009.
(32) Tomasi, J.; Mennucci, B.; Cammi, R. *Chem. Rev.* **2005**, *105*, 2999.
(33) Grimme, S. *J. Comput. Chem.* **2006**, *27*, 1787.
(34) Rehr, J. J.; Albers, R. C. *Rev. Mod. Phys.* **2000**, *72*, 621.
(35) Newville, M. *J. Synchrotron Radiat.* **2001**, *8*, 322.
(36) Sheehan, S. W.; Thomsen, J. M.; Hintermair, U.; Crabtree, R. H.; Brudvig, G. W.; Schmuttenmaer, C. A. *Nat. Commun.* **2015**, *6*, 6469.
(37) Thomsen, J. M.; Huang, D. L.; Crabtree, R. H.; Brudvig, G. W. *Dalton Trans.* **2015**, *44*, 12452.
(38) Diaz-Morales, O.; Hersbach, T. J. P.; Hetterscheid, D. G. H.; Reek, J. N. H.; Koper, M. T. M. *J. Am. Chem. Soc.* **2014**, *136*, 10432.
(39) Gilbert, J. A.; Eggleston, D. S.; Murphy, W. R.; Geselowitz, D. A.; Gersten, S. W.; Hodgson, D. J.; Meyer, T. J. *J. Am. Chem. Soc.* **1985**, *107*, 3855.
(40) Yang, X.; Baik, M.-H. *J. Am. Chem. Soc.* **2006**, *128*, 7476.
(41) Liu, F.; Concepcion, J. J.; Jurss, J. W.; Cardolaccia, T.; Templeton, J. L.; Meyer, T. J. *Inorg. Chem.* **2008**, *47*, 1727.

DOI: 10.1021/jacs.6b01750
J. Am. Chem. Soc. 2016, 138, 5511−5514